Proceedings of the ASME 2011 30th International Conference on Ocean, Offshore and Arctic Engineering
OMAE2011
June 19-24, 2011, Rotterdam, The Netherlands

OMAE2011-49955

OPTIMIZATION OF MOORING CONFIGURATION PARAMETERS OF FLOATING WAVE ENERGY CONVERTERS

Pedro C. Vicente*
IDMEC,
Instituto Superior Técnico,
Technical University of Lisbon,
Lisbon, Portugal

António F. O. Falcão
IDMEC,
Instituto Superior Técnico,
Technical University of Lisbon,
Lisbon, Portugal

Paulo A. P. Justino
Laboratório Nacional de Energia
e Geologia,
Lisbon, Portugal

ABSTRACT

Floating point absorbers devices are a large class of wave energy converters for deployment offshore, typically in water depths between 40 and 100m. As floating oil and gas platforms, the devices are subject to drift forces due to waves, currents and wind, and therefore have to be kept in place by a proper mooring system.

Although similarities can be found between the energy converting systems and floating platforms, the mooring design requirements will have some important differences between them, one of them associated to the fact that, in the case of a wave energy converter, the mooring connections may significantly modify its energy absorption properties by interacting with its oscillations. It is therefore important to examine what might be the more suitable mooring design for wave energy devices, according to the converters specifications.

When defining a mooring system for a device, several initial parameters have to be established, such as cable material and thickness, distance to the mooring point on the bottom, and which can influence the device performance in terms of motion, power output and survivability.

Different parameters, for which acceptable intervals can be established, will represent different power absorptions, displacements from equilibrium position, load demands on the moorings and of course also different costs.

The work presented here analyzes what might be, for wave energy converter floating point absorber, the optimal mooring configuration parameters, respecting certain pre-established acceptable intervals and using a time-domain model that takes into account the non-linearities introduced by the mooring system.

Numerical results for the mooring forces demands and also motions and absorbed power, are presented for two different mooring configurations for a system consisting of a hemispherical buoy in regular waves and assuming a liner PTO.

NOMENCLATURE

a	radius of floater
a_f	radius of submerged floater in case II
A	added mass
A_w	wave amplitude
B	radiation damping coefficient
C	damping coefficient of PTO
f_d	diffraction or excitation force
g	acceleration of gravity
h_1	vertical distance of the submerged floater to the bottom in static conditions
H	water depth
l	length of the mooring cable sections
L_0	length of the bottom-mooring cable laying on the bottom in static conditions
L_1	distance between the contact point at the seabed and the buoy centre (for case I) or the submerged floater centre (for case II)
L_2	distance between the submerged floater centre and centre of the buoy in case II
m	mass of buoy
m_f	mass of submerged floater
P_{avg}	time-averaged power
t	time
v_f	volume of the submerged floater

* Author of correspondence

x, z	displacements from mean position of body centres (buoy and submerged floater) (Fig. 1)
x_{Max}	maximum horizontal displacement
ρ	density

Subscripts

B	buoy
LHS, RHS	cable on the left and right hand side of the buoy
f	floater
x, z	directions of x, z axes

INTRODUCTION

Among the wide variety of floating wave energy devices, point absorbers have been object of special development effort since the late 1970s. They are oscillating bodies whose horizontal dimensions are small in comparison with the representative wavelength. Examples of devices are the IPS buoy [1], Aquabuoy [2], Wavebob [3] and PowerBuoy [4]. Their rated power ranges typically from tens to hundreds of kW.

Floating point absorbers, as any floating object, are subject to drift forces due to waves, currents and wind, and so they have to be kept on station by moorings. However, their mooring design has an important requirement, since, for a wave energy converter, the mooring connections may interact with its oscillations, which might significantly modify its energy absorption properties. It is therefore important to explore what might be the most suitable mooring design according to the converter and location placement specifications.

When defining a mooring system for a device, several initial parameters have to be established, such as cable material and thickness, distance to the mooring anchor on the bottom, and so on. Different configurations will represent different displacements from the equilibrium position for the converter, load demands on the moorings and power absorbed.

In the work presented here we investigate in some detail the influence that some of the mooring system parameters can have on the performance of the converters, specifically in terms of power absorbed and horizontal displacement.

MATHEMATICAL MODEL

A wide range of different options exist when designing a mooring system, but two main classes can be defined: slack chain and taut synthetic lines. Slack chain lines rely on their weight to provide the necessary horizontal restoring force and, although they induce some vertically downward force, they allow for systems with a lower stiffness than the ones with taut synthetic lines. In this work we will considerer the mooring system of a floating point absorber with slack chains lines.

We consider a hemispherical buoy, moored to the bottom by catenary lines, as shown in plan view in Fig. 1, for two different configurations, a single cable (case I – blue line) and a cable with an intermediary submerged floater (case II – green lines). Cables in a symmetric configuration are placed to the right-hand side of the buoy.

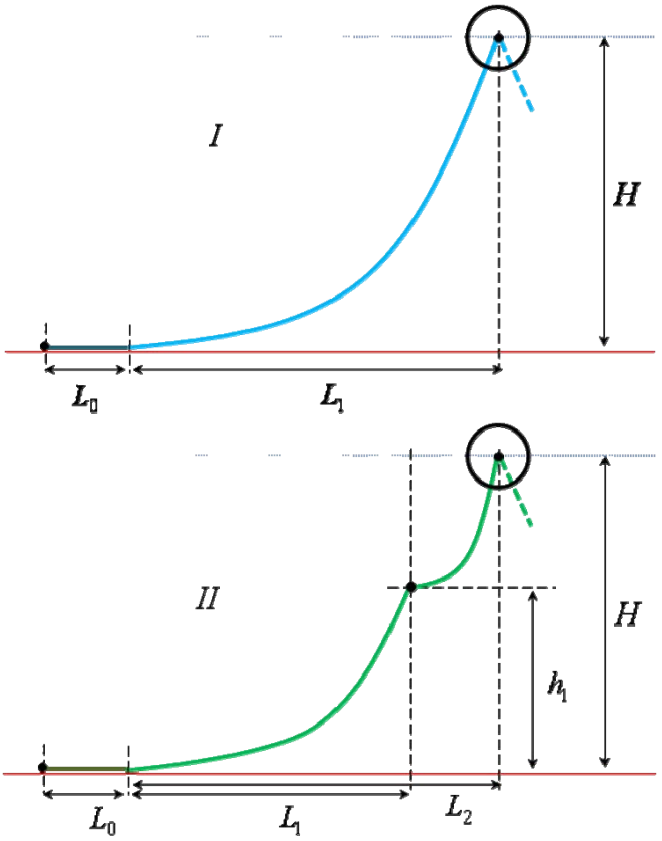

Figure 1 – Plane view of the mooring configurations, a single cable (case I – blue line) and a cable with a intermediary submerged floater (case II – green lines).

In this analysis the slack mooring cables are approximately modelled as catenary lines in a quasi-static analysis. Also, although it may introduce some imprecision in the model, in order to have it somewhat simplified, the cables are assumed inelastic and their dynamic effects (namely cable inertia and viscous drag forces) are ignored; but not the submerged cable weight per unit length W , which depends on the cable material used (chain, wire, fibre) and its construction [5].

In this way the classical catenary equations [6] apply, which can be written as

$$Z = \left(\frac{T_H}{W}\right)\cosh\left(\frac{D}{T_H/W}+\alpha\right)+\beta \qquad (1)$$

$$s = \left(\frac{T_H}{W}\right)\sinh\left(\frac{D}{T_H/W}+\alpha\right)+\gamma \qquad (2)$$

$$T = T_H\cosh\left(\frac{D}{T_H/W}+\alpha\right) \qquad (3)$$

$$T_V = T_H \sinh\left(\frac{D}{T_H / W} + \alpha\right) \tag{4}$$

Here, D and Z are the horizontal and vertical coordinates of the cable point with respect to the lowest point of the catenary (where the cable departs from the bottom); α, β and γ are constants which are determined from boundary conditions; s is the length of the catenary-shaped part of the cable; T is the tension force at the cable point, and T_H and T_V its horizontal and vertical components. Finally W is the submerged cable weight (cable weight minus buoyancy force) per unit length.

The boundary conditions at the point of seabed contact are $s = 0$, $D = 0$, $Z = 0$, $dZ/dD = 0$ and at the buoy $Z = H$ and $D = L_1$ (for case I) or $D = L_2$ (for case II). In case II, at the submerged floater, the boundary conditions are such that $D = L_1$, $Z = h_1$ and

$$\left.\frac{dZ}{dD}\right|^{+} - \left.\frac{dZ}{dD}\right|^{-} = \frac{P_f}{T_H} \tag{5}$$

where P_f is a force upwards (since the submerged body is less dense than water) that is equal to the difference between the floater weight and its buoyancy force

$$P_f = m_f g - v_f \rho_0 g = v_f (\rho_f - \rho_0) g \tag{6}$$

From these boundary conditions it is possible to calculate, for the initial equilibrium position, the initial horizontal cable tension T_H (which is equal for all points of the cable) and, from this, T_V and T for any specific point in the cable.

It is also possible to calculate the floater radius (in case II) and the hanging cable length s, which in turn allows to calculate the cable length l of each section ($l = s + L_0$ for the cable connected to the anchor point on the bottom and $l = s$ for the hanging cable in case II). It is also easy to calculate the initial horizontal and vertical mooring tensions applied to the floater in case II, R_H and R_V, respectively.

Since, in calm sea, the centre of the hemispherical buoy (of radius a) is supposed to lie on the free-surface plane, the buoy mass m must be

$$m = \frac{2}{3}\pi a^3 \rho - \frac{1}{g} 2T_V \tag{7}$$

Note that, since the buoy centre is assumed to lie on the free-surface horizontal plane in static conditions, the mass m of the moored buoy slightly varies with the mooring configuration parameters for case I and II, since it is dependent on T_V.

TIME DOMAIN ANALYSIS

The buoy and the submerged floater, acted upon by the waves and mooring lines, are made to oscillate in heave and horizontally. The displacements of their centre from their mean position is defined by the coordinates (x_j, z_j) with $j = B$ for the buoy and $j = f$ for the submerged floater, where x is the horizontal coordinate (pointing to the right), and z is a vertical coordinate pointing upwards.

The dynamic equations for the buoy are then

$$\begin{aligned}(m + A_{\infty x})\ddot{x}_B(t) + \int_{-\infty}^{t} L_x(t-\tau)\ddot{x}_B(t)d\tau \\ = f_{dx_B} + T_{X,\,RHS} - T_{X,\,LHS}\end{aligned} \tag{8}$$

$$\begin{aligned}(m + A_{\infty z})\ddot{z}_B(t) + \rho g S z_B(t) + \int_{-\infty}^{t} L_z(t-\tau)\ddot{z}_B(t)d\tau \\ = f_{dz_B} - C\dot{z}_B - (T_{Z,\,RHS} + T_{Z,\,LHS}) + (2T_V)\end{aligned} \tag{9}$$

Here, $A_{\infty u}$ $(u = x, z)$ are the limiting values of the added masses $A_u(\omega)$ for $\omega = \infty$. For a hemispherical floater, it is $A_{\infty z} = \mu/2$ and $A_{\infty x} = 0.2732\mu$, where $\mu = 2\pi a^3 \rho / 3$ (see [7]). f_{dx} and f_{dz} are the horizontal (x) and vertical (z) components of the wave excitation force on the buoys (see [8]).

The power take-off system (PTO) of the floating converter is assumed to consist of a simple linear damper activated by the buoy heaving motion. The vertical force it produces on the buoy is $-C\dot{z}_B$. Finally, $S = \pi a^2$.

The convolution integrals in Eqs. (8-9) represent the memory effect in the radiation forces. Their kernels can be written as

$$L_u(t) = \frac{2}{\pi}\int_{-\infty}^{t} \frac{B_u(\omega)}{\omega} \sin \omega t \, d\omega \quad (u = x, z) \tag{10}$$

They decay rapidly and may be neglected after a few tens of seconds, which means the infinite interval of integration in Eqs. (8-9) may be replaced by a finite one in the numerical calculations (a 20s interval was adopted as sufficient). The integral-differential equations (8-9) were numerically integrated from given initial values of x, z, $\dot{x}$ and $\dot{z}$, with an integration time step of 0.05 s.

$B_u(\omega)$ $(u = x, z)$ are the frequency-dependent hydrodynamic coefficients of radiation damping concerning the horizontal (subscript x) and heave (subscript z) oscillation modes of the spherical buoy.

T_V is, as already mentioned, the initial vertical cable tension applied to the converter, at equilibrium position. The time varying values of the mooring forces $T_{X,v}$ and $T_{Z,v}$ on each cable, on the left-hand side ($v = LHS$) and right-hand side ($v = RHS$) of the converter, are calculated based on the position of the buoy ($F = T$ and $j = B$) at each instant of time, and considering the cable lengths l defined for the static position. For case II, it is necessary to take into account also the submerged floater ($j = f$) and the tension forces ($F = R$) applied to it. In both cases, similar catenary equations as before for the equilibrium position apply

$$Z + z_j = \left(\frac{F_{X,v}}{W}\right)\cosh\left(\frac{D \pm x_j}{F_{X,v}/W} + \alpha\right) + \beta \qquad (11)$$

$$s = \left(\frac{F_{X,v}}{W}\right)\sinh\left(\frac{D \pm x_j}{F_{X,v}/W} + \alpha\right) + \gamma \qquad (12)$$

The plus or minus sign is used according to the cable considered is on the right or left side of the buoy.

The submerged floater is subject to the pulling forces of the mooring lines connected to it, its own weight, the buoyancy force and the hydrodynamic forces on it. For this case, similar dynamic equations to the ones of the buoy apply

$$(m_f + A_{\infty fh})\ddot{x}_f(t) + \int_{-\infty}^{t} L_{fh}(t-\tau)\ddot{x}_f(t)d\tau = f_{d\,fx} + R_{fX,RHS} - R_{fX,LHS} \qquad (13)$$

$$(m_f + A_{\infty fz})\ddot{z}_f(t) + \int_{-\infty}^{t} L_{fz}(t-\tau)\ddot{z}_f(t)d\tau = f_{d\,fz} + \left(R_{fZ,RHS} + R_{fZ,LHS}\right) - \left(2R_V\right) \qquad (14)$$

The kernels of the convolution integrals L_{fu} $(u = x,z)$ are calculated as before, considering $B_{fu}(\omega)$ $(u = x,z)$ as the hydrodynamic coefficients of radiation damping of the floater. $f_{d\,fx}$ and $f_{d\,fz}$ are the horizontal and vertical components of the wave excitation force on the floater.

In this case, the effects of the wave radiation and diffraction induced by the buoy upon the floaters were neglected. For the added mass $A_{\infty\,fu}$ $(u = x,z)$, we take the added mass of an accelerating sphere in an unbounded fluid (see e.g. [9]) $A_{fx} = A_{fz} = (2/3)\rho\pi a_f^3$.

NUMERICAL RESULTS

We set $\rho = 1025$ kg.m^{-3} (sea water density) and $g = 9.8$ ms^{-2}. The submerged floater is a sphere of density $\rho_f = 50$ kg.m^{-3}. The floaters submergence is assumed to be sufficient for the excitation force and the radiation damping on them to be neglected, i.e. we set $B_{fx} = B_{fz} = 0$ and $f_{d\,fx} = f_{d\,fz} = 0$.

In all cases for which results are shown here (except where clearly stated otherwise), it is $a = 7.5$ m, $L_0 = 0.65 \times L_1$ for case I and $L_0 = 0.65 \times L_2$ for case II, $L_1 = 50$ m, $L_2 = 80$ m, $h_1 = 45$ m and $C = 251.1$ kN/(m/s). A value for the submerged cable weight of $W = 1520$ N/m was used, adequate for example for a 90mm thick chain cable (see [5]). The adopted value of $C = 251.1$ kN/(m/s) is obtained from defining $C = B$, and is the one that allows maximum wave energy absorption by an isolated unmoored hemispherical heaving buoy, at resonance frequency (see e.g. [8]).

In regular waves the excitation force components are assumed to be simple-harmonic functions of time and so we may write $\{f_{dx}, f_{dz}\} = \mathrm{Re}\left(\{F_{dx}, F_{dz}\}e^{i\omega t}\right)$, where the complex amplitudes F_{dx} and F_{dz} are proportional to the amplitude A_w of the incident wave. The moduli of F_{dx} and F_{dz} may be written as $\{|F_{dx}|, |F_{dz}|\} = \{\Gamma_x A_w, \Gamma_z A_w\}$, where $\Gamma_x(\omega)$ and $\Gamma_z(\omega)$ are (real positive) excitation force coefficients.

Deep water was assumed for the hydrodynamic coefficients of added mass, radiation damping and excitation force. The frequency dependent numerical values for the spherical buoy were obtained with the aid of the boundary element code WAMIT, for the radiation damping coefficients $B_u(\omega)$ and the absolute value $\Gamma_u(\omega)$ and phase $\arg\left(F_{dz}(\omega)/F_{dx}(\omega)\right)$ of the excitation forces coefficients, for the floating hemispheres, oscillating horizontally and vertically $(u = x, z)$.

Here we perform an initial investigation, on the influence of the mooring system parameters, $\{L_1, W\}$ for case I and $\{L_1, h_1, L_2\}$ for case II. This was done, on the one hand, on the average power by the converter P_{avg} and, on the other hand, on the maximum horizontal displacement x_{Max}, which in turn can be related to the tension demands placed on the buoy and can affect the system survivability. We take into account different water depths H.

Some numerical results are illustrated in Figs. 2 and 3 for case I and in Figs. 4 to 6 for case II, for regular waves of $A_w = 1$ m and $T = 10$ s.

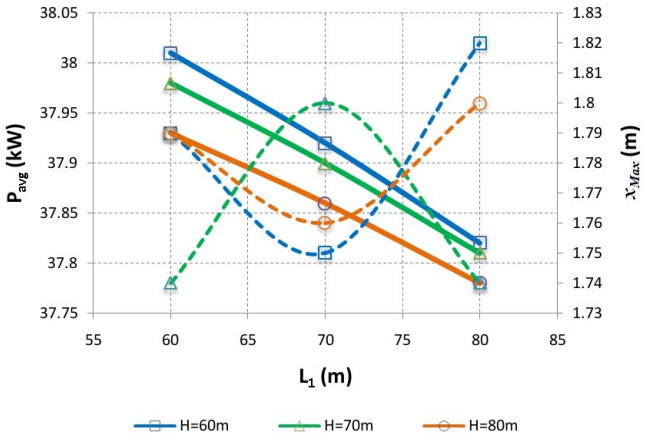

Figure 2 – For case I, influence of the horizontal distance between the buoy and the anchor point L_1, in terms of average power P_{avg} (straight line) and maximum surge displacement x_{Max} (dashed line), for different water depths H and W=1520N/m.

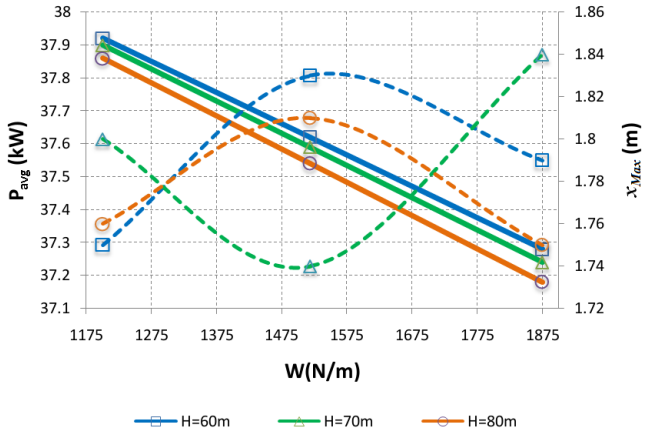

Figure 3 – For case I, influence of the cable submerged weight W in terms of average power P_{avg} (straight line) and maximum surge displacement x_{Max} (dashed line) for different water depths H and L_1=70m.

For case I, it can be seen that the mooring parameters affect the system performance, even if only to some extent. This influence is better observed in the maximum horizontal displacement (dashed line) than in the absorbed power (straight line). For the power absorbed, the dependence appears to be linearly proportional, but the same cannot be said of the horizontal displacement, with a non linear variation both with the mooring parameters and the water depth.

For case II, it can be seen that, unlike in case I, the dependency of the power absorbed on the mooring parameters and water depth appears to be non linear. Also, the mooring parameters in this case seem to have a stronger influence on the performance of the system. The mooring configuration of case II seems to indicate that a bigger amount of power absorption is possible to be achieved and with a smaller horizontal displacement, although perhaps at the cost of longer cable.

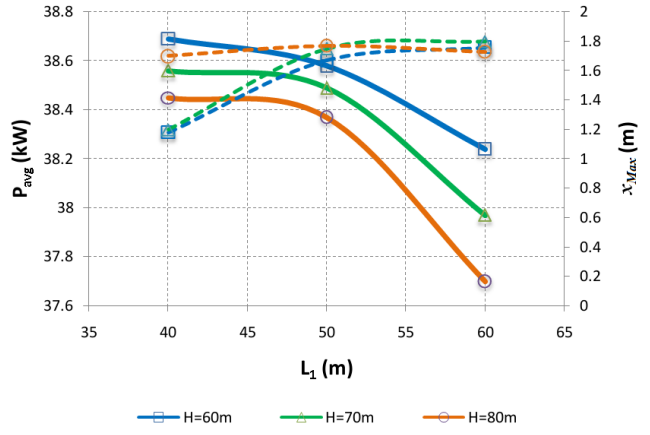

Figure 4 – For case II, influence of the horizontal distance between the buoy and the submerged floater L_1, in terms of average power P_{avg} (straight line) and maximum surge displacement x_{Max}, (dashed line) for different water depths H and for W=1520N/m , L_2=80m *and* h_1=45m.

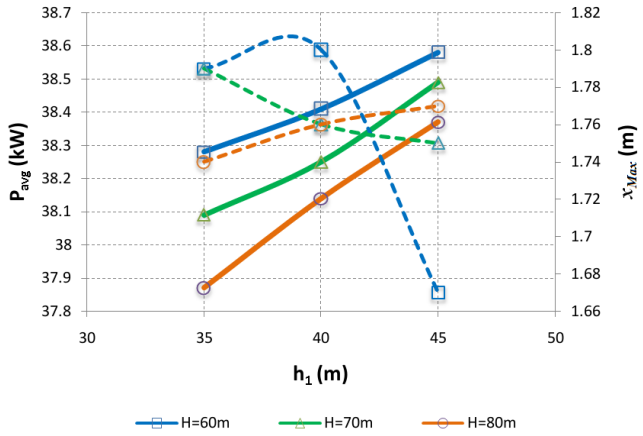

Figure 5 – For case II, influence of the submerged floater vertical distance to bottom h_1 , in terms of average power P_{avg} (straight line) and maximum surge displacement x_{Max} (dashed line), for different water depths H and for W=1520N/m , L_1=50m and L_2=80m.

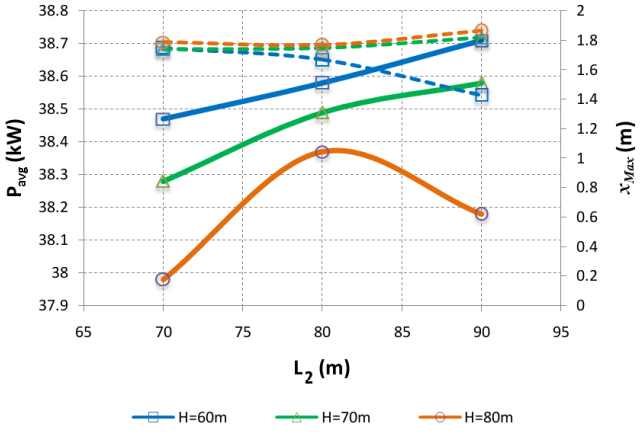

Figure 6 – For case II, influence of the horizontal distance between the buoy and the anchor point L_2 , in terms of average power P_{avg} (straight line) and maximum surge displacement x_{Max} (dashed line), for different water depths H and for W=1520N/m , L_1=50m and h_1=45m.

This initial analysis with different discrete values of the parameters gave some indication of their influence for the different water depths H considered. The next step was to analyze, for a given water depth, which group of mooring parameters appears to be better both for maximizing the power absorbed and minimizing the horizontal displacement of the converter. The results of this analysis can be observed in Figs. 7 and 8 for case I and in Figs. 9 to 11 for case II, again for regular waves of $A_w = 1$ m and $T = 10$ s.

It can be seen that, as indicated in Figs. 2 and 3, for case I, there is an approximately linear dependency on the power absorbed with the mooring parameters considered. The maximum power absorption appears to be achieved for smaller distances to the anchor point and lighter chain cables and with these values still allowing for smaller maximum horizontal

displacements. As could be expected, a light chain introduces a smaller vertically downwards force on the buoy and therefore allows for larger vertical displacement and as a result higher power absorption. Also the non linear dependency of the horizontal displacement is clearly seen.

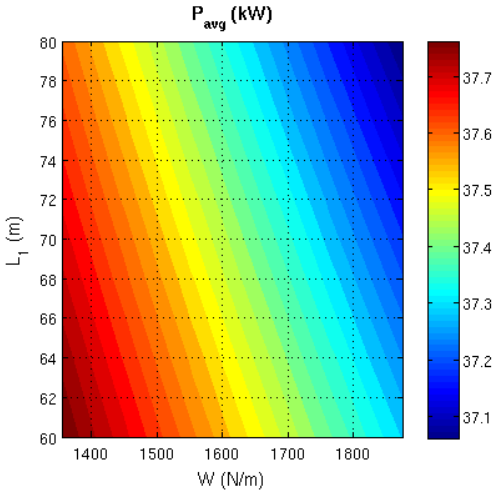

Figure 7 – For case I, influence of the horizontal distance between the buoy and the anchor point L_1 and the cable submerged weight W on the average absorbed power P_{avg}, for H=80m.

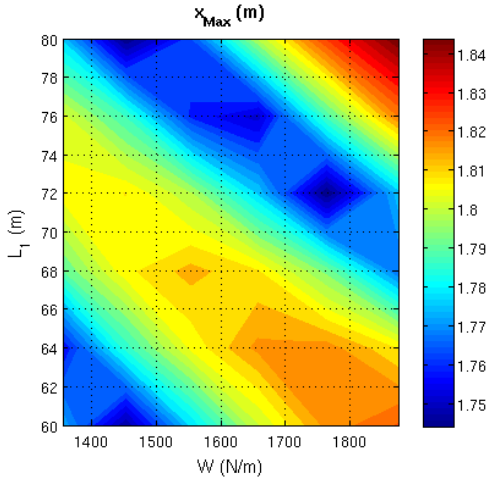

Figure 8 – For case I, influence of the horizontal distance between the buoy and the anchor point L_1 and the cable submerged weight W on the maximum horizontal displacement x_{Max}, for H=80m.

For case II, the non linear dependency of the power absorbed and the horizontal displacement on all the mooring parameters can be clearly seen. These results give some suggestions on which might be the best group of mooring parameters to both maximize power and minimize displacement. For the submerged floater, and for the intervals considered, a higher vertical distance from the bottom h_1, a smaller distance to the mooring point L_1 and a bigger distance to the buoy, seem to be more suitable for higher power absorption and smaller horizontal displacement. It can also be seen that some pairs or group of parameters are not adequate since they yielded invalid or unstable results (the areas in the graphs which are in white).

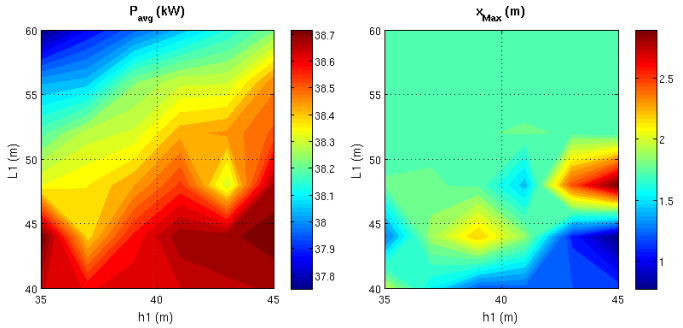

Figure 9 - For case II, influence of the horizontal distance between the anchor point and the submerged floater L_1 and of its vertical distance to the bottom h_1, on the average absorbed power P_{avg} and on the maximum horizontal displacement x_{Max}, for H=80m and L_2=80m.

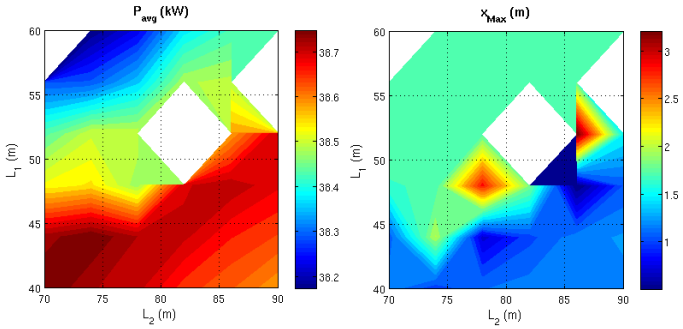

Figure 10 – For case II, influence of the horizontal distance between the anchor point and the submerged floater L_1 and the anchor point and the buoy L_2, on the average absorbed power P_{avg} and on the maximum horizontal displacement x_{Max}, for H=80m and h_1=45m.

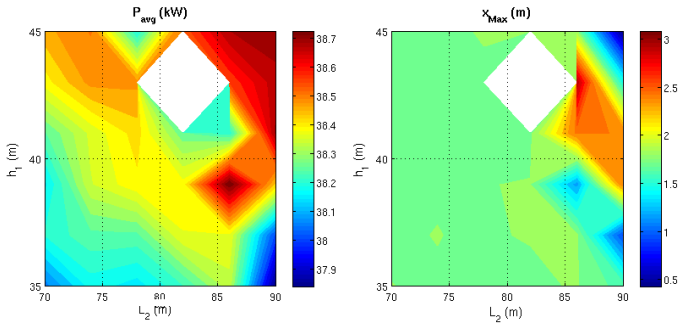

Figure 11 – For case II, influence of the horizontal distance between the anchor point and the buoy L_2 and its vertical distance to the bottom h_1, on the average absorbed power P_{avg} and on the maximum horizontal displacement x_{Max}, for H=80m and L_1=50m.

CONCLUSIONS

A theoretical analysis of the influence of the mooring system parameters on the power absorbed and horizontal oscillations of a slack moored wave energy converter was

presented. Two different cases are analyzed of slack chain mooring lines, with and without an additional submerged floater. A time-domain analysis was applied to examine the effects of the mooring lines on the system performance.

Numerical results were obtained for a hemispherical buoy whose PTO consists of a linear spring and a linear damper. The analysis focused on the amplitude of the horizontal motion and power absorbed by the converter, for the two mooring configurations considered.

Slack chain catenary lines rely on their weight to provide the necessary horizontal restoring force and, although they induce some vertically downward force, they were found not to affect very significantly the power absorption in the proposed configurations.

An initial analysis revealed that the system behaviour was influenced by the mooring parameters although only to a limited extent. In case I, concerning a single mooring line, for the power absorbed the dependence appears to be of linear proportionality, but the same cannot be said of the horizontal displacement. In case II, concerning the mooring lines with submerged floater, the dependencies are clearly non linear.

Further analysis indicated which group of mooring parameters appears to be better for both maximizing the power absorbed and minimizing the horizontal displacement.

The initial analysis presented here, which focused on some of the mooring parameters and was done only for regular waves, is to be extended to irregular waves. It would also be interesting to look for a direct relationship between what might be the optimal mooring parameters and the floater radius and the local water depth. A further step could be to resort to an optimization algorithm program that would define, for the systems considered, the optimal group of parameters that would either maximize the power absorbed or minimize the horizontal displacement or even both.

ACKNOWLEDGMENTS

The work reported here was partly supported by the Portuguese Foundation for Science and Technology under contracts PTDC/EME-MFE/103524/2008, POCI-SFA. . The first author wants to thank the sponsorship of the MIT-Portugal doctoral programme.

REFERENCES

[1] L. Cleason, J. Forsberg, A. Rylander, B.O. Sjöström. Contribution to the theory and experience of energy production and transmission from the buoy-concept. Proc. 2nd Int. Symp. Wave Energy Utilization. Trondheim, Norway, 1982, p. 345-370.

[2] A. Weinstein, G. Fredrikson, M.J. Parks, K. Nielsen. Aquabuoy, the offshore wave energy converter numerical modelling and optimization. Proc. MTTS/IEEE Techno-Ocean ’04 Conf., Kobe, Japan, 2004, vol. 4, p. 1854-1859.

[3] http://www.wavebob.com/

[4] http://www.oceanpowertechnologies.com/

[5] I. Johanning, G.H. Smith, J. Wolfram. Mooring design approach for wave energy converters. Proc. Inst. Mech. Eng. Part M-J. Eng. Marit. Environ., vol. 220, p. 159-174, 2006.

[6] R.J. Smith, C.J. MacFarlane. Statics of a three component mooring line. Ocean Eng., vol. 28, p. 899-914, 2001.

[7] A. Hulme. The wave forces acting on a floating hemisphere undergoing forced periodic oscillations. J. Fluid Mech., vol. 121, p. 443-463, 1982.

[8] J. Falnes. Ocean Waves and Oscillating Systems. Cambridge University Press, Cambridge, 2002.

[9] J. Lighthill. An Informal Introduction to Theoretical Fluid Mechanics. Oxford University Press, Oxford, 1986.